Protection of Pancreatic β-Cells from Various Stress Conditions Is Mediated by DJ-1*S

Alex Inberg[‡1] **and Michal Linial**[‡§2]

From the ‡Department of Biological Chemistry and §Sudarsky Center for Computational Biology, Hebrew University of Jerusalem, Jerusalem 91904, Israel

Pancreatic β-cells are vulnerable to multiple stresses, leading to dysfunction and apoptotic death. Deterioration in β-cells function and mass is associated with type 2 diabetes. Comparative two-dimensional gel electrophoresis from pancreatic MIN6 cells that were maintained at varying glucose concentrations was carried out. An induced expression of a protein spot, detected in MIN6 cells experiencing high glucose concentration, was identified by mass spectrometry as the oxidized form of DJ-1. DJ-1 (*park7*) is a multifunctional protein implicated in familial Parkinsonism and neuroprotection in response to oxidative damage. The DJ-1 protein and its oxidized form were also induced following exposure to oxidative and endoplasmic reticulum stress in MIN6 and βTC-6 cells and also in mouse pancreatic islets. Suppression of DJ-1 levels by small interfering RNA led to an accelerated cell death, whereas an increase in DJ-1 levels by adenovirus-based infection attenuated cell death induced by H_2O_2 and thapsigargin in β-cell lines and mouse pancreatic islets. Furthermore, DJ-1 improved regulated insulin secretion under basal as well as oxidative and endoplasmic reticulum stress conditions in a dose-dependent manner. We identified TFII-I (*Gtf2i*) as DJ-1 partner in the cytosol, whereas the binding of TFII-I to DJ-1 prevented TFII-I translocation to the nucleus. The outcome was attenuation of the stress response. Our results suggest that DJ-1 together with TFII-I operate in concert to cope with various insults and to sustain pancreatic β-cell function.

The decreasing number of functional pancreatic β-cells, combined with a malfunction of the remaining ones, is known to be a major contributor to the development and progression of diabetes mellitus type 2 (type 2 diabetes; T2D)[3] (1).

Throughout the course of the disease, the detrimental influence of high glucose levels and free fatty acids affects β-cell functionality and survival. These processes, called "glucotoxicity" and "lipotoxicity," frequently act synergistically, and are referred to as "glucolipotoxicity" (2). In pancreatic β-cells, the main mechanism by which glucotoxicity decreases the cellular functionality is based on the excessive production of reactive oxygen species (ROS). ROS levels are even further amplified when the processes of glucotoxicity and lipotoxicity coincide (3).

Several pathways participate in the disruption of β-cell functionality by oxidative stress. The activity of Pdx1, a major pancreatic transcription factor, is directly influenced by ROS levels. That, in turn, affects the expression of critical genes for carbohydrate homeostasis (4). In accordance with these observations, treatment with antioxidant substances and overexpressing antioxidant enzymes greatly improve β-cell functionality and viability (5). An additional critical factor in maintaining β-cell functionality is the ability to cope with ER stress (6, 7). The pathways by which pancreatic β-cells respond to ER stress ultimately result in a decrease in protein synthesis, selective induction of stress-related proteins, and apoptosis (8).

The sensitivity of cells to stress, and specifically to oxidative and ER stress, is common to neurodegenerative and metabolic diseases (9, 10). A tight connection between oxidative stress and neurodegeneration is exhibited by the function of DJ-1. DJ-1 is a multifunctional protein that was shown to be responsible for the early onset of Parkinson disease (PD) (11). DJ-1 is associated with numerous functions (reviewed in Ref. 12). In the context of PD, DJ-1 was proposed to act as a chaperone to prevent α-synuclein fibrillation (13). DJ-1 is believed to act as a sensor for oxidative stress and as an antioxidant protein (14) capable of *in vivo* and *in vitro* quenching of ROS (15). Overexpression of DJ-1 in the brain improves cellular viability under oxidative stress, whereas DJ-1 knockdown mice exhibit an increased susceptibility to oxidative reagents (16, 17). DJ-1 is a regulator of androgen receptor-dependent transcription, an oncogene with a strong cell-growth promoting activity, and plays a role in fertilization (18). DJ-1 affects cell survival by cooperating with Ras (19) and is implicated in key signaling cascades, such as PTEN, phosphatidylinositol 3-kinase, and Akt (20). Serving as a transcriptional co-activator, DJ-1 stabilizes the activity of a master regulator of response to oxidative stress, NRF2 (21) and sequesters Daxx to the nucleus, thus preventing apoptosis (22). Despite this wealth of data, the exact mechanism underlying the involvement of DJ-1 in various cellular processes remains to be fully elucidated.

[3] The abbreviations used are: T2D, type 2 diabetes; BiP, Ig-binding protein; BSA, bovine serum albumin; ER, endoplasmic reticulum; FACS, fluorescence-activated cell sorting; GFP, green fluorescence protein; MS, mass spectrometry; MALDI, matrix-assisted laser desorption ionization; TOF, time-of-flight; PD, Parkinson disease; PI, propidium iodide; ROS, reactive oxygen species; shRNA, small hairpin RNA; CHAPS, 3-[(3-cholamidopropyl)-dimethylammonio]-1-propanesulfonic acid; MTT, 3-(4,5-dimethylthiazol-2-yl)-2,5-diphenyltetrazolium bromide; KRB, Krebs-Ringer bicarbonate buffer.

Here we present cellular and molecular evidence suggesting the role of DJ-1 in oxidative and ER stress management in pancreatic β-cells. We show that DJ-1 expression increases as a result of excessive growth conditions, such as high glucose, oxidative stress, and ER stress. We show that DJ-1 improves viability and functionality of β-cells in a dose-dependent manner in cell lines and in pancreatic islets. We identify TFII-I (GTF2i) as a partner of DJ-1 in the cytosol and show that the binding of DJ-1 to TFII-I defines the accessibility of TFII-I to engage transcription. We propose that DJ-1 and TFII-I constitute a critical junction in physiological stress coping pathways in pancreatic β-cells. We postulate that DJ-1 and its direct partners may be involved in the pathogenesis of T2D.

EXPERIMENTAL PROCEDURES

Antibodies and Cell Culture—Antibodies used in this study include polyclonal DJ-1 (Bethyl Laboratories), TFII-I, and BiP (Santa Cruz Biotechnology, Inc. (Santa Cruz, CA)); monoclonal antibodies were for actin, β-tubulin (Santa Cruz Biotechnology, Inc.) and FLAG (Chemicon Laboratories). Secondary antibodies (Jackson Immunoresearch) were coupled to horseradish peroxidase or to fluorescence dyes (Cy3 and Cy5).

Mouse pancreatic β-cell line MIN6 and βTC-6 were generously provided by Prof. M. Walker (Weizmann Institute of Science) and Prof. S. Efrat (Tel-Aviv University), respectively. Both cell lines are characterized by their glucose-dependent insulin release (23, 24). MIN6 cells were maintained in monolayer in 11 mM glucose Dulbecco's modified Eagle's medium complemented with 15% fetal calf serum and 50 μM β-mercaptoethanol. MIN6 cells used were from 26–35 cell passages. βTC-6 cells were maintained in Dulbecco's modified Eagle's medium complemented with 25 mM glucose and 10% fetal calf serum. Cell passages 28–35 were used for the above cells. All cell lines were equilibrated with 5% CO_2 at 37 °C and supplemented with 50 mg/liter streptomycin and 75 mg/liter penicillin sulfate. Cell culture reagents were from Biological Industries Co. (Beit Haemek, Israel).

Isolation of mouse islets of Langerhans was supported by Dr. Yuval Dor (Hadassah Medical School) and was performed according to regulation and animal care ethical protocols. Islets of Langerhans were isolated from C57BL/6 mice by ductal perfusion with collagenase P. The intact islets were handpicked and maintained in RPMI medium supplemented with 10% fetal calf serum for 48 h prior to the experiment. About 1.5×10^5 cells were analyzed for each experiment.

Islet Disruption—Freshly harvested islets were allowed to recover for 24 h in RPMI medium supplemented with 10% fetal calf serum. The islets then were transferred into Hanks' buffered salt solution without Mg^{2+} and Ca^{2+} supplemented with 2 mM EGTA. The islets were incubated in 37 °C with delicate agitation every 5 min. Following 20 min, the EGTA-containing medium was replaced with the RPMI medium containing AdDJ or AdBL adenovirus using a similar multiplicity of infection.

DNA Constructs—The adenovirus-based expression system for expression of DJ-1 mouse protein (AdDJ and AdBL vectors) was constructed based on the AdEasy system (25). All of the components were generously provided by Dr. Bert Vogelstein (The Johns Hopkins University). In short, the complete cDNA sequence of the mouse *park7* gene with an addition of FLAG tag on the C terminus was cloned into the pAdTrack-CMV shuttle vector. Following the recombination of the shuttle vector with the pAdEasy-1 adenovirus backbone vector in BJ5183 cells, the resulting recombinant vectors were screened using PCR, indicative digestion, and partial sequencing. The positive clones were used to generate the adenoviruses using HEK-293T cells. The same procedure was used to construct the control GFP-only-producing AdBL adenovirus. In order to create the L166P mutation adenovirus, the cDNA sequence of mouse DJ-1 was subjected to site-directed mutagenesis using QuikChange (Stratagene), and the correct nucleotide replacement was verified by sequencing. The mutated sequence was used to create the AdL166P adenovirus as described above.

Small interfering RNA down-regulation of DJ-1 in MIN6 cells was done by establishing a stable cell clone carrying a small hairpin RNA (shRNA)-expressing vector. DJ-1 shRNA was inserted in pRNAT-U6.1/Neo (GeneScript; supplemental Fig. S1) and controlled by the U6 promoter. shRNA DJ-1 plasmid was transfected to MIN6 using Lipofectamine 2000 (Invitrogen). Stable clones were selected using 600 μg/ml G418 (Invitrogen) for 4 weeks.

Antibody-based Detection—The cells were lysed in ice-cold radioimmune precipitation buffer (25 mM Tris-HCl, pH 7.6, 150 mM NaCl, 1% Nonidet P-40, 1% sodium deoxycholate, 0.1% SDS) with mammalian protease inhibitor mixture (Sigma). The sample protein concentration was measured using a BCA protein assay kit (Pierce), and equal quantities were loaded onto an SDS-polyacrylamide gel. Following the electrophoresis, standard Western blotting protocol including detection using an enhanced chemiluminescence detection kit (EZ-ECL, Biological Industries) was applied (26). For immunofluorescence detection, cells were grown on glass coverslides, fixed with 4% paraformaldehyde, and incubated with the appropriate secondary antibodies conjugated with fluorescent dyes Cy3 and Cy5 (Jackson Immunoresearch). The cultures were visualized using an Eclipse TI S/L-100 inverted microscope (Nikon).

Fluorescence Microscopy of Live Islets—In order to assess the expression of DJ-1 in adenovirus-infected disrupted islets, the GFP that is used as a marker in the adenovirus construct was visualized using an Eclipse TI S/L-100 inverted microscope (Nikon).

Co-Immunoprecipitation—50% confluent MIN6 cells were infected with AdDJ adenovirus. Following 48 h, the cell lysates were prepared as above. Cell lysates was cleared by centrifugation (20 min, 12,000 × *g*). Pull-down was performed using EZ-View anti-FLAG beads (Sigma) according to the manufacturer's protocol. The precipitates were washed three times with the lysis buffer prior to eluting the proteins using 100 μg/ml FLAG peptide (F4799, Sigma). The eluted proteins were separated using 8–20% SDS-polyacrylamide gels, visualized using Bio-Safe colloidal Coomassie stain (Bio-Rad), excised, and analyzed by MALDI-TOF as described.

Two-dimensional Gel Electrophoresis—MIN6 cells and mouse pancreatic islets were lysed in the isoelectric focusing sample buffer consisting of 7 M urea, 2 M thiourea, 4% CHAPS, 40 μM dithiothreitol, and 2% (v/v) ampholites (pH 3–10). The

samples were solubilized using an ultrasonic bath (10 min) followed by gentle vortex for 1 h at room temperature. The samples were centrifuged by 15 min at 15,000 $\times$ g, and the supernatants were collected. The protein concentration was determined using RC-DC protein assay (Pierce).

Immobilized pH gradient strips with a length of 18 cm and pH range of 3–10 were used for most experiments. In the case of mouse pancreatic islets, 7-cm pH 3–10 strips were used. The sample was introduced to the strips using the active in-gel sample rehydration technique. The dry strips were placed in the focusing tray (IEE, Bio-Rad) for 12 h, and 50 V were applied on each strip. Following the rehydration, the isoelectric focusing was performed according to the standard protocols. In brief, gradient voltages were applied on the strips, until total V-h values reached 15,000 V-h or 80,000 V-h in 7- or 18-cm immobilized pH gradient strips, accordingly. Following the IEF, the focused strips were removed from the focusing tray and equilibrated in order to solubilize the proteins and to reduce the disulfide bonds. The strips were placed first in buffer containing 50 mM Tris-HCl, pH 6.8, 6 M urea, 30% (v/v) glycerol, 2% (w/v) SDS, and 2% (w/v) dithiothreitol for 10 min in order to reduce the S–S bonds. Afterward, the strips were placed for 10 min in similar buffer, containing 2.5% (w/v) iodoacetamide instead of dithiothreitol. Following the reduction/alkylation step, the strips were placed on top of 12% SDS-polyacrylamide gels, sealed with 1% low melting agarose solution, and run until the tracking dye reached the bottom of the gel. Prior to mass spectrometry analysis, the gels were fixed using 12% acetic acid, 50% ethanol solution and stained using Coomassie Brilliant Blue G-250 colloidal stain with subsequent destaining in water. All of the materials and reagents used for 2-DE were purchased from Bio-Rad.

Mass Spectrometry (MS) Analysis—The gel spots from SDS-polyacrylamide gels were cut out of the gel as 1–1.5-mm diameter gel plugs and cut to smaller pieces using a scalpel. The gel plugs were destained two times with 200 μl of 200 mM ammonium bicarbonate (NH_4HCO_3), pH 8.0, and mixed 1:1 with acetonitrile for 45 min at 37 °C, and then the gel pieces were dried in SpeedVac. The dry gel pieces were rehydrated in 10 μl of 0.02 μg/μl sequencing grade modified trypsin (Promega) in 10% acetonitrile, 40 mM NH_4HCO_3 pH 8.0, for 1 h at room temperature to allow the trypsin solution to diffuse into the gel pieces. If needed, the gel pieces were covered with 50 μl of 10% acetonitrile, 40 mM NH_4HCO_3, pH 8.0, to prevent them from drying. The gel pieces were incubated for 16–18 h at 37 °C. Following the digestion, the solution was removed and put in a fresh 0.5-ml tube. 50 μl of 0.1% trifluoroacetic acid were added to the gel pieces and sonicated for 15 min. The solution was removed and combined with one from the previous step. The combined solution was dried using a SpeedVac and resuspended in ~10 μl of 0.1% trifluoroacetic acid and then desalted and concentrated using a ZipTip (Millipore) reversed phase microcolumn according to the manufacturer's instructions.

MALDI-TOF MS analysis was performed on a Bruker Daltonics MICROFLEX mass spectrometer. All measurements were performed in positive ion/reflectron mode using standard working protocols. For peptide measurements, α-cyano-4-hydroxycinnamic acid was used as a matrix, utilizing the dried droplet technique. In brief, 0.5 μl of sample solution was mixed with a similar volume of the saturated α-cyano-4-hydroxycinnamic acid solution in 30% acetonitrile, 0.1% trifluoroacetic acid, spotted on a stainless steel MALDI target, and allowed to dry. The mass measurements were performed according to instructions, with trypsin autodigestion peaks used as internal calibrants. The monoisotopic peptide masses were identified using the Bruker TOF Analysis software. The peptide masses were sent to the MASCOT searching software (Matrix Science, London, UK) using the Bruker BioTools software. The NCBI non-redundant protein database was used for searching, with search parameters including methionine oxidation, iodoacetamide modification of cysteines, trypsin digestion with one missed cleavage, and 50 ppm mass error window. Only unambiguously identified proteins above the statistically significant threshold scores were considered.

Cell Viability and Insulin Release—Following the exposure to various stressors, cell viability was assessed using the 3-(4,5-dimethylthiazol-2-yl)-2,5-diphenyltetrazolium bromide (MTT) assay in 96-well plates. The cells were incubated in medium containing 1 mg/ml MTT until dark formazan crystals were visible under a microscope (~1 h). The cells were washed with phosphate-buffered saline and solubilized using 200 μl of DMSO, and the absorbance was measured using a wavelength of 570 nm in a microplate reader. For each experiment, 5–8 replicates were used per concentration in the case of cell lines and triplicates in the case of mouse pancreatic islets. Each experiment was repeated three times with similar results.

Cell death was also measured by fluorescence-activated cell sorting (FACS). Cells were incubated with membrane-impermeant propidium iodide (PI), an indicator of cell death. MIN6 cells were incubated with PI (1 μg/ml) for 5 min and analyzed on a BD FACSCalibur flow cytometer. Measurements were collected for 10 min by exciting with a 488-nm line and collecting fluorescence emission at a 620-nm filter. Following 24 h, PI fluorescence was measured in untreated cells and those exposed to 200 μM H_2O_2.

For insulin release, MIN6 cells were grown in 24-well plates at ~75% confluence. The cells were washed once with Krebs-Ringer bicarbonate buffer (KRB; 119 mM NaCl, 4.74 mM KCl, 1.19 mM KH_2PO_4, 1.19 mM $MgCl_2$, 25 mM $NaHCO_3$, 10 mM HEPES, pH 7.4, and 2.54 mM $CaCl_2$) supplemented with 0.5% bovine serum albumin. The cells were preincubated with KRB/BSA supplemented with 5 mM glucose for 30 min, washed with KRB/BSA, and incubated in KRB/BSA for 60 min supplemented with various glucose concentrations. Following the glucose stimulation, the medium was collected, and the insulin secreted was evaluated using the Ultrasensitive Mouse ELISA kit (Mercodia). The amount of secreted insulin was normalized to the viable cell number in each well.

RESULTS

Induction of DJ-1 in Pancreatic β-Cells—A comparative study on pancreatic mouse insulinoma MIN6 cells using two-dimensional gel electrophoresis was performed on cells that were maintained at varying glucose levels for 7–10 days. Such conditions mimic the physiological glucose load in prediabetic
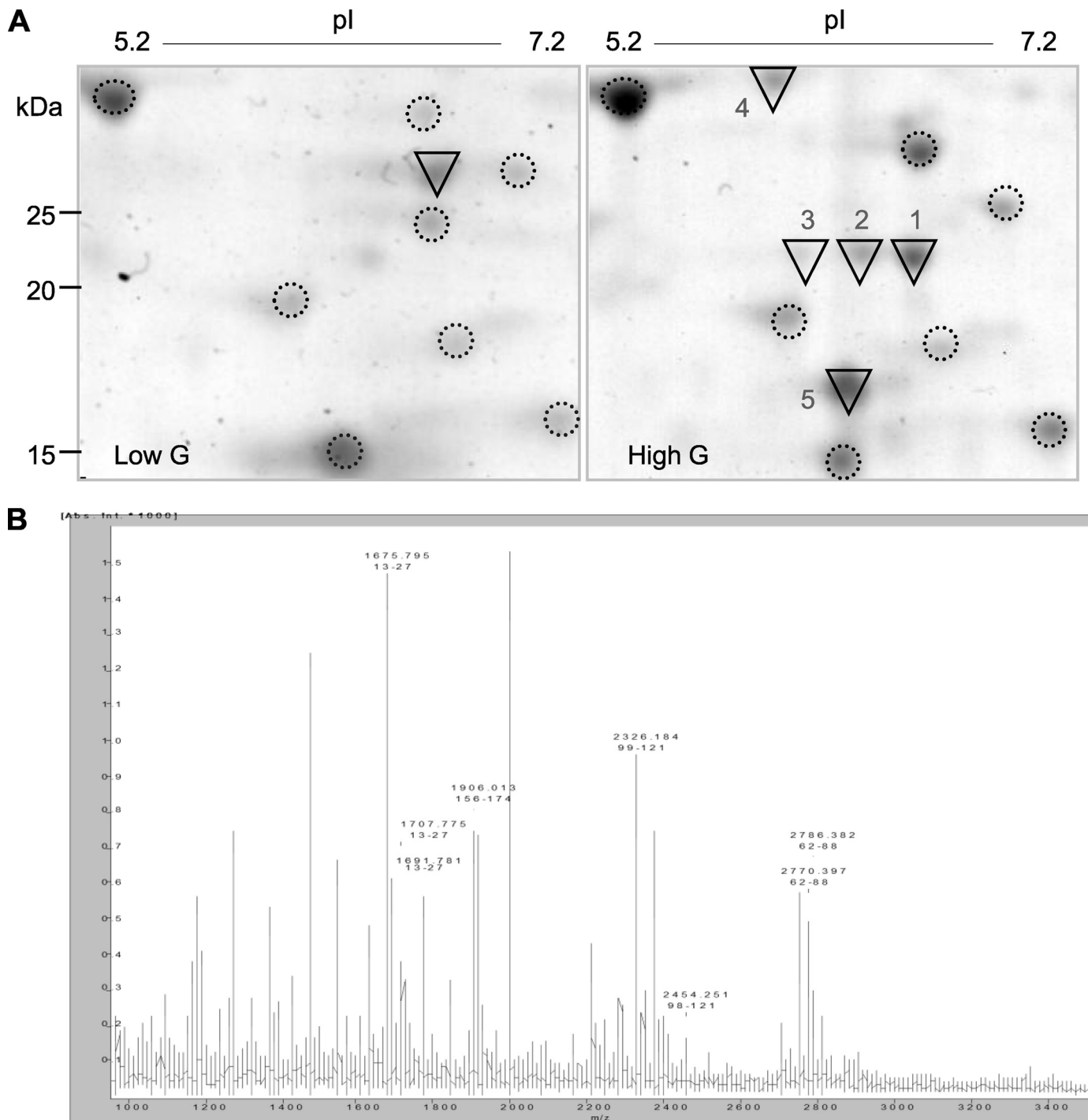
FIGURE 1. **DJ-1 expression at high glucose and following oxidative stress.** *A*, MIN6 cells maintained at 5 mM (*Low G*) or 25 mM glucose (*High G*) for 7 days were collected and subjected to two-dimensional gel electrophoresis. A section of the gels is shown, and spots that are expressed to a similar level (<1.5-fold differential expression ratio) are *aligned* and *circled* (*dashed line*). The spots that were induced or repressed >2-fold at high G are marked by *triangles*. Spots 1–5 were identified by MALDI-TOF MS (see "Mass Spectrometry (MS) Analysis" section of "Experimental Procedures"). *B*, MALDI-TOF spectra of DJ-1. The confidently identified peptides are marked. Extended MS identification data are given in supplemental Table S1 and supplemental Fig. S2.

pancreatic islets. The two-dimensional gel electrophoresis gels of cells that were maintained at 5 mM glucose and at 25 mM glucose were compared (Fig. 1*A*, low and high glucose, respectively). Although most proteins showed no difference in expression under these conditions (Fig. 1*A*, *circled*), the expression of a number of low molecular weight proteins (15–35 kDa) was changed (Fig. 1*A*, *triangles*). We focused on the proteins that were induced at high glucose growth conditions (Fig. 1*A*, *num-*

bered). Using MALDI-TOF MS, we identified the following highly induced proteins: (i) proteasome β7 subunit precursor (Fig. 1*A*, *triangle 4*; UniProt: P70195) (this protein is a subunit of the proteasome that carries the trypsin-like activity) and (ii) peptidylprolyl isomerase A (UniProt: P17742; Fig. 1*A*, *triangle 5*) (this protein accelerates the folding of proteins by catalyzing the isomerization of prolines in oligopeptides). Furthermore, we consistently noted two new spots of ~22 kDa that were not

A

B

C
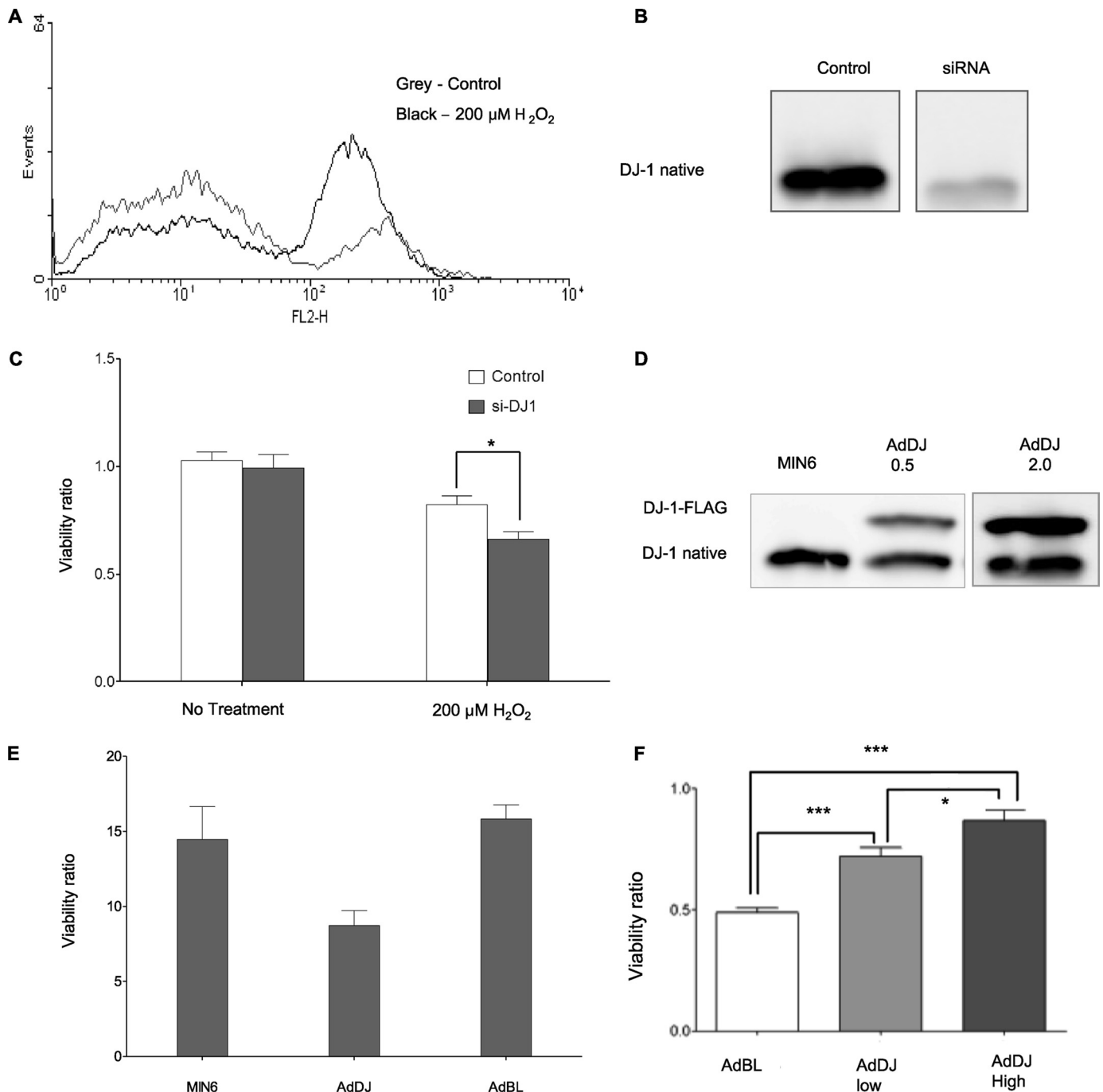

D

E

F
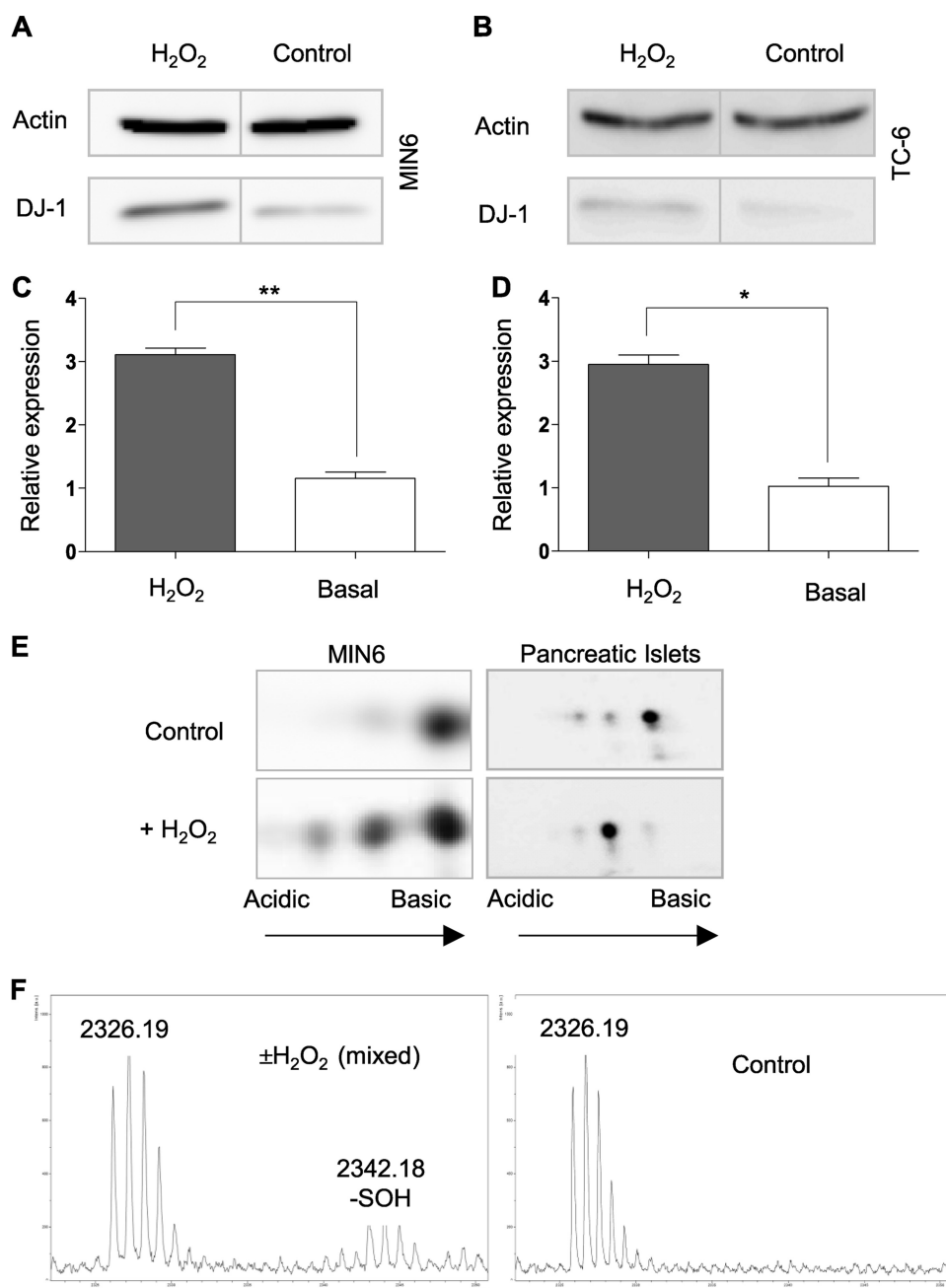
FIGURE 2. **Quantitative analysis for DJ-1.** Shown is Western blot using anti DJ-1 antibodies in MIN6 (*A*) and βTC-6 cells (*B*) in untreated state and following treatment with 200 μM H_2O_2. Results of three experiments are shown with mean $\pm$ S.E. (*error bars*). Significance is measured according to Student's *t* test (*, $p < 0.05$) for MIN6 (*C*) and βTC-6 cells (*D*). *E*, two-dimensional gel electrophoresis analysis by DJ-1 antibodies of two-dimensional gel electrophoresis from MIN6 and mouse pancreatic islets from untreated basal state and following treatment with 200 μM H_2O_2 for 6 and 2 h, respectively. Shown are sections of the gels covering pI 5.5–6.5 (marked *Acidic* to *Basic*) and size range of 20–25 kDa. *F*, spots from two-dimensional gel electrophoresis experiments using MIN6 (as in Fig. 1*B*) were subjected to further analysis. Shown are MALDI-TOF spectra of the peptide GLIAAI-CAGPTALLAHEVGFGCK (amino acids 99–121; Cys[106] is underlined). *Right*, MS spectrum of the basic isoform (pI 6.4, 2326.19 Da); *left*, MS spectrum of the 1:1 ratio of the basic and the acidic form (marked *mixed*). A sulfenic acid-modified peptide is present with a mass reflecting cysteine carrying a -SOH group (2342.18 Da).

In neurons, DJ-1 was shown to respond to oxidative stress and to numerous toxic insults (15). Using DJ-1 antibodies, we quantified the change in the overall DJ-1 expression in MIN6 (Fig. 2*A*) and βTC-6 (Fig. 2*B*) following exposure to H_2O_2 oxidative stress. Exposure of the cells to H_2O_2 caused a nearly 3-fold increase in total DJ-1 protein levels (Fig. 2, *C* and *D*) and 2.6-fold increased expression from mice pancreatic islets (not shown).

In order to further characterize the different DJ-1 isoforms identified by the mass spectrometry, we set out to test the possibility that DJ-1 serves as an oxidative sensor in pancreatic β-cells using two-dimensional gel electrophoresis and specific DJ-1 antibodies. Under basal conditions, a basic form (with pI of ~6.4) dominates DJ-1 expression in MIN6. A similar observation is valid for isolated mice pancreatic islets (Fig. 2*E*, *top*). Incubating the cells and the islets with H_2O_2 (Fig. 2*E*, *bottom*) revealed two additional spots with a lower pI (6.1 and 5.8). In pancreatic islets, the shift toward the main acidic form (pI 6.1) occurred within 2 h, and the fraction of the modified form reached ~90% of the DJ-1 level. MIN6 under the same conditions showed a consistent shift that reached only ~45% of the total DJ-1 in MIN6 cells (Fig. 2*E*). Using MALDI-TOF MS, we further investigated the DJ-1 spots that were induced following high glucose exposure in MIN6 cells (Fig. 1*A*, spots marked *2* and *3*). We validated these additional modified spots to be cysteine-sulfenic acid oxidized forms. According to the identified mass differences, we identified a tryptic peptide that matches a sulfenic modification (Fig. 2*F*, *left*). The sequence of DJ-1 contains 4 cys-

teines that are prone to modifications under oxidative conditions (supplemental Fig. S2). We had identified the oxidation modifications by monitoring the change in the calculated peptide mass (supplemental Table S1). Cysteine oxidation was identified in the peptide containing Cys[106], the residue that is most prominently subjected to cysteine-sulfinic modifications in cells exposed to various toxic agents (27).

seen in two-dimensional gels under low glucose growth conditions (Fig. 1*A*, *triangles 2* and *3*), whereas protein number 1 was substantially induced. We identified these three spots as DJ-1, a multifunctional protein that was implicated in familial PD. The tryptic peptides that were confidently identified by MASCOT are shown (Fig. 1*B*). See supplemental Table S1 and supplemental Fig. S2 for detailed information.
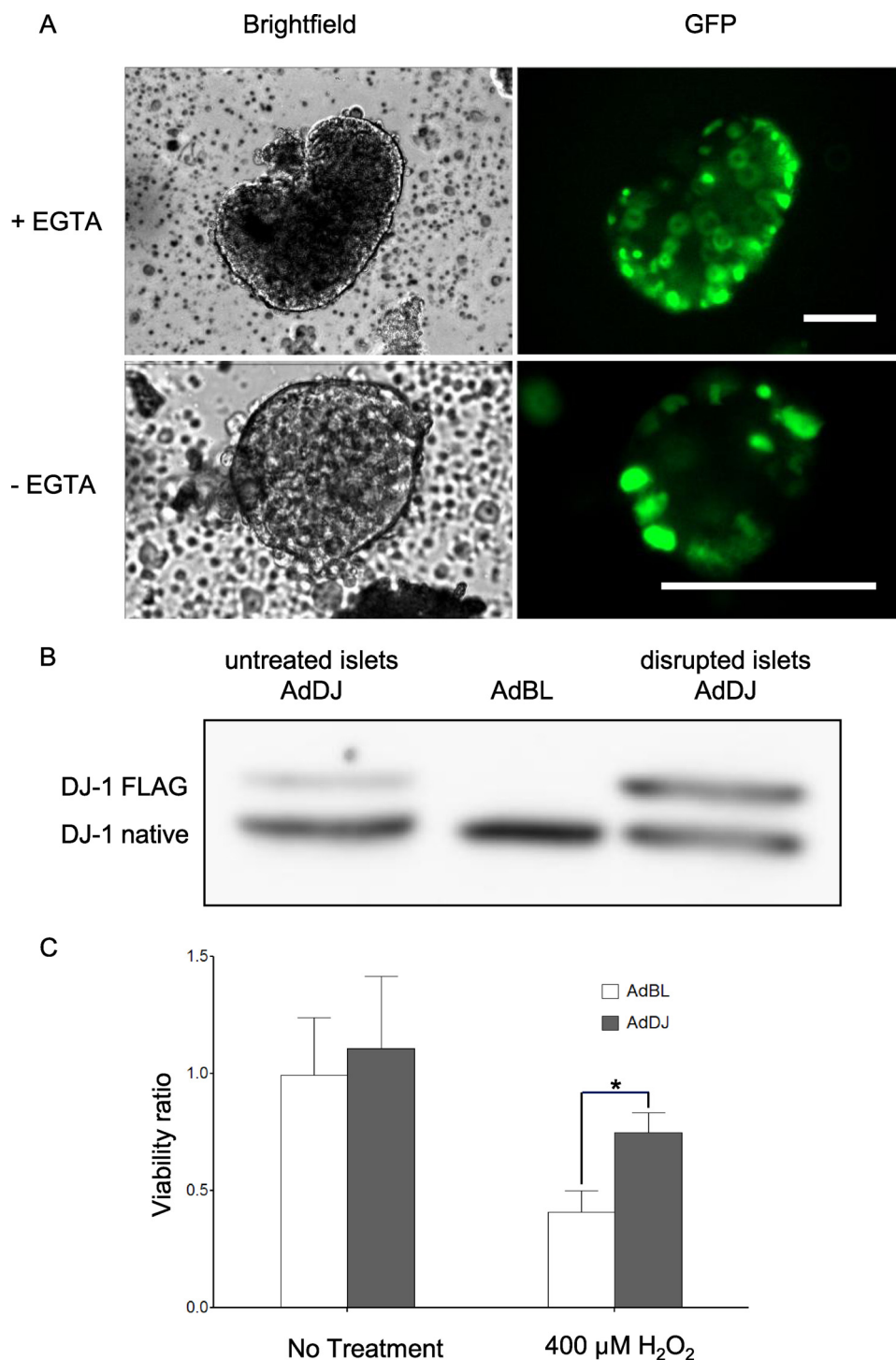
FIGURE 3. **DJ-1 improves survival of MIN cells.** *A*, FACS analysis of MIN6 stained by PI, an indicator of cell death. MIN6 cells were incubated with PI (1 μg/ml), and the intensity of the fluorescence was monitored relative to control, untreated culture. The elevation in the fluorescence intensity in MIN6 following 200 μM H_2O_2 is shown by the *black line* (compare with the *gray line* curve). The degree of PI-positive cells ranges was 17% (ranged from 12 to 22%). *B*, Western blot analysis of DJ-1, indicating the down-regulation by small interfering RNA DJ-1 (*si-DJ1*). *C*, cell survival was assessed using an MTT assay in the presence of 200 μM H_2O_2. *D*, Western blot analysis of FLAG-tagged DJ-1 expressed using AdDJ vector and analyzed using DJ-1 antibodies. The exogenous DJ-1 shows a higher molecular weight due to the addition of the FLAG tag. The AdDJ-expressed DJ-1 level relative to the endogenous levels was measured. Examples for moderate expression and high expression indicate an addition of 50 and 200% levels of the FLAG-tagged exogenous DJ-1 (marked *0.5* and *2.0*, respectively). *E*, viability FACS analysis of AdDJ- and AdBL-infected MIN6 cells following oxidative stress (200 μM H_2O_2) as stained with PI (1 μg/ml). *F*, cell survival was assessed using an MTT assay in the presence of 400 μM H_2O_2. Cells expressed infected wild type DJ-1 (AdDJ) at a level of 50% (low) and 100% (high) addition relative to the endogenous level. Values are means ± S.E. (*error bars*), representative to 5–8 replicates. Significance is measured according to Student's *t* test (*, $0.01 < p < 0.05$; ***, $p < 0.001$).

DJ-1 Attenuates Cell Death under Stress Conditions—Various studies have previously described the protective role of DJ-1 in neuronal cells under various stress conditions (16, 28). In order to assess the influence of DJ-1 on β-cell viability and functionality, we tested the MIN6 cells while manipulating the levels of DJ-1 in cells. To test the sensitivity of MIN6 to H_2O_2 oxidative stress, we measured cell viability using PI by a cell sorter (Fig. 3*A*). At 200 μM H_2O_2 ~17% of the cells were identified as necrotic. This fraction of PI-positive cells is in agreement with the tetrazole-based MTT assay (Fig. 3*B*). Both assays

A

Brightfield | GFP

+ EGTA

− EGTA

B

untreated islets
AdDJ | AdBL | disrupted islets
AdDJ

DJ-1 FLAG
DJ-1 native

C

FIGURE 4. **Cell survival is improved in pancreatic islets overexpressing DJ-1 following oxidative stress.** *A*, purified mouse pancreatic islets overexpressing DJ-1, followed by adenoviral infection, as indicated by the GFP expression 48 h postinfection. Partial disruption by EGTA (+ *EGTA*) or nontreated (− *EGTA*) islets is marked. *Scale bar*, 100 μm. *B*, Western blot analysis of DJ-1 expression in EGTA-disrupted or untreated mouse islets infected with AdDJ and AdBL adenovirus. *C*, cell survival in AdDJ-infected mouse pancreatic islets following oxidative stress. 48 h postinfection, the cells were exposed to 400 μM H_2O_2 and assayed 12 h later. The cell viability was examined using the MTT assay as described. Values are means ± S.E. (*error bars*). Significance is measured according to Student's *t* test (*, $p < 0.05$).

that expressed DJ-1 shRNA (for a detailed sequence, see supplemental Fig. S1). Stably expressing shRNA DJ-1 clones were selected using G418. A clone in which the basal level of DJ-1 was reduced by ~2.5-fold (Fig. 3*B*, *si-DJ1*) showed an enhanced cell death under stress conditions induced by 200 μM H_2O_2 (Fig. 3*C*). To further substantiate the potential protective role of DJ-1 in cell survival, we conducted overexpression experiments using the adenovirus-based gene delivery system with the benefit of titrating the expression levels and reaching a preferred level of exogenous tagged protein. FLAG-tagged DJ-1 protein-expressing adenovirus (AdDJ) and blank FLAG-only-expressing adenovirus (AdBL) were produced. Cells that were further analyzed following infection expressed 50–300% additional DJ-1 relative to the endogenous levels (Fig. 3*D*). Using DJ-1 antibodies, we tracked the endogenously and exogenously expressing DJ-1 and estimated the additional expression levels to be 50 and 200% (marked *AdDJ 0.5* and *2.0*, respectively). Using FLAG antibodies, we monitored the cellular localization of the exogenously expressed DJ-1. No apparent difference in localization of the tagged DJ-1 when compared with staining by antibody against DJ-1 was seen.

We used the cell sorting assay (as in Fig. 3*A*) to monitor the impact of DJ-1 on cell survival under oxidative stress (200 μM). DJ-1-infected cells (AdDJ) show a significantly reduced fraction of PI positive cells when compared with blank FLAG-only expressing adenovirus (AdBL) (Fig. 3*E*). To better evaluate the degree of such apparent protection from oxidative stress, the cell viability was assessed using the tetrazole-based MTT assay following treatment with 400 μM H_2O_2. We show that 24 h following treatment, the cell survival of the all DJ-1-infected cells was significantly improved (Fig. 3*F*) in a dose-dependent manner.

In order to further substantiate the survival improvement observed in cell lines and to place this finding in the physiologic context, the influence of DJ-1 expression on the oxidative stress

were used to quantify the viability of the cells following various stressors.

Knockdown and overexpression of DJ-1 were achieved by the small interfering RNA- and adenovirus-based infection technologies, respectively. We established a stable cell line of MIN6
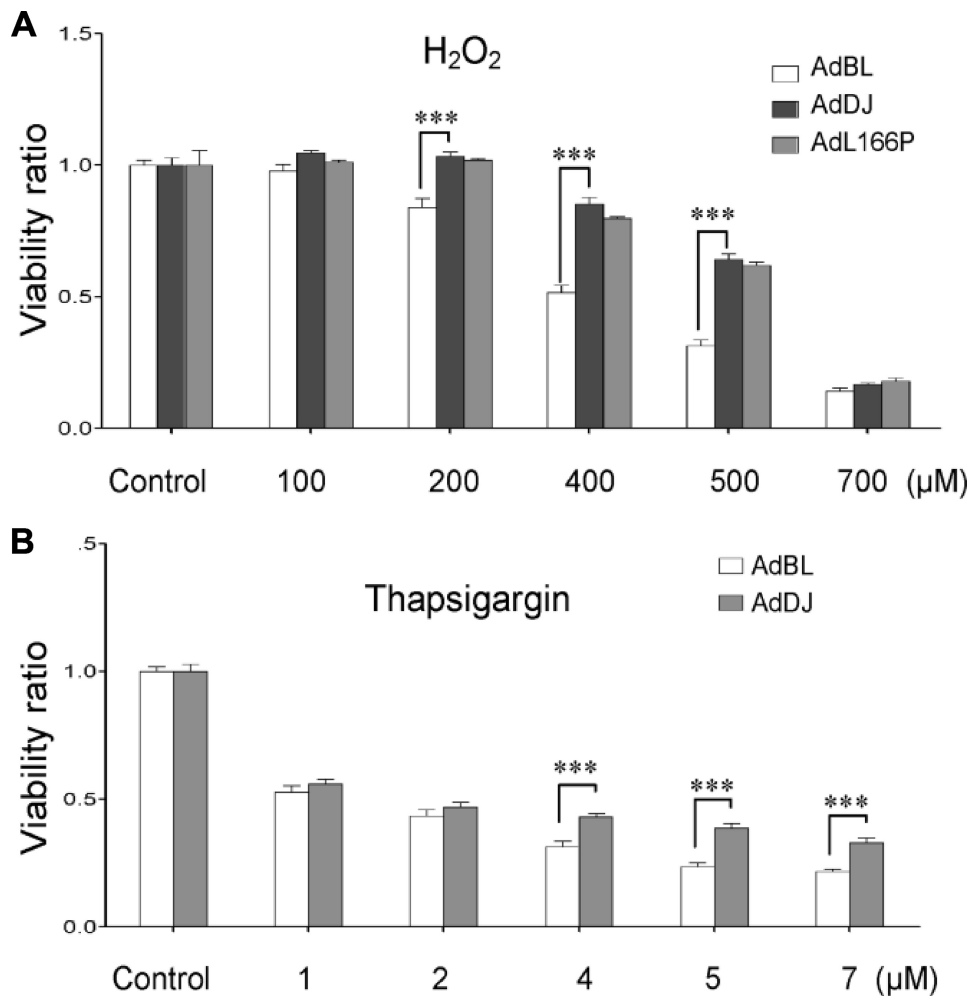
A

B

FIGURE 5. **Cell survival assay in cells overexpressing DJ-1.** *A*, MIN6 cells are infected with adenovirus carrying DJ-1 at a level of 100% addition to the wild type (AdDJ), L166P-mutated DJ-1 (AdL166P), and blank virus (AdBL). 48 h postinfection, the cells were exposed to the indicated concentrations of H_2O_2 or thapsigargin (*B*) for 1 h and assayed 24 h later. Results shown are representative from three independent experiments. Values are means ± S.E. (*error bars*), representative of 5–8 replicates. Significance is measured according to Student's *t* test (*, $0.01 < p < 0.05$; **, $0.001 < p < 0.01$; ***, $p < 0.001$).

amounts). We recorded a significant protection against cell death at a range of 200–500 μM H_2O_2. We prepared a FLAG-tagged DJ-1 bearing the L166P mutation adenovirus (AdL166P). This mutation was identified in early onset of PD and was attributed to DJ-1-impaired stability (11). Introducing DJ-1 with an L166P mutation (AdL166P) to the cells at the same levels (the addition of 100% infected DJ-1) resulted in a beneficial effect similar to that of the wild type DJ-1 under a wide range of concentrations of H_2O_2 (Fig. 5*A*).

The expression of DJ-1 was induced following the exposure to high glucose (Fig. 1) and in response to oxidative stress (Fig. 2). We tested whether other modes of stress may lead to an induction in DJ-1 protein expression. To this end, we tested the response of the pancreatic cells to ER stress conditions using thapsigargin as a stressor. Thapsigargin is an ER Ca^{2+}-ATPase blocker that induces ER stress. We show that DJ-1 is induced by 2-fold in MIN6 cells and by ~3-fold in βTC-6 cells (supplemental Fig. S3).

To assess the potential of DJ-1 to improve cell survival under ER stress conditions, we performed similar experiments (as in Fig. 5*A*), using a range of thapsigargin concentrations. We show that DJ-1 overexpression in MIN6 improves cell viability under ER stress at a range of thapsigargin concentrations that caused already substantial damage to cell viability (Fig. 5*B*, cell death >60%). The beneficial effect, as in the case of oxidative stress, was dose-dependent. We conclude that the beneficial effect of DJ-1 on cell viability applies at a range of stressor concentrations and is manifested also under extreme oxidative and ER stress conditions (Fig. 5).

DJ-1 Improves Regulated Insulin Release—It is widely accepted that oxidative stress impairs glucose-induced insulin release in pancreatic β-cells. Because proper insulin release can serve as an indication of β-cell functionality, we measured the glucose-dependent insulin secretion of the DJ-1-expressing MIN6 cells. AdBL-infected cells were subjected to various glucose concentrations, and insulin release was compared with the uninfected cells (Fig. 6*A*). We thus rule out the influences of the adenoviral infection *per se* on the glucose-induced insulin release. A substantial improvement in insulin release at 25 mM glucose concentration in the DJ-1-overexpressing cells was shown prior to any external stress (Fig. 6*B*). The cells were exposed to oxidative stress using different concentrations of H_2O_2, and the insulin

sensitivity of mouse pancreatic islets was assessed (Fig. 4). Using the adenoviral expression system, we overexpressed DJ-1 in freshly harvested whole mouse islets. Because direct islet infection by adenoviral expression vectors is limited by the islet anatomical structure, the expression results are often partial and unstable. We therefore utilized a protocol for a partial islet disruption by EGTA that substantially improves the accessibility of the adenovirus and the efficiency of DJ-1 expression. Although untreated islets show only limited infection of the peripheral cells, the EGTA-disrupted islets are prone to a substantial infection, and the overexpression of DJ-1 is validated (Fig. 4, *A* and *B*). In AdDJ-infected pancreatic islets that overexpressed DJ-1, we measured an improvement in viability following treatment with 400 μM H_2O_2 (Fig. 4*C*). Those results are in accord with the cell line viability results (Fig. 3), further establishing the physiological basis of the findings.

We tested the improvement of DJ-1-induced cell protection toward multiple stressors (Fig. 5). Gradual concentrations of H_2O_2 were tested on cells with a constant level of modestly overexpressed DJ-1 (100% relative to endogenous
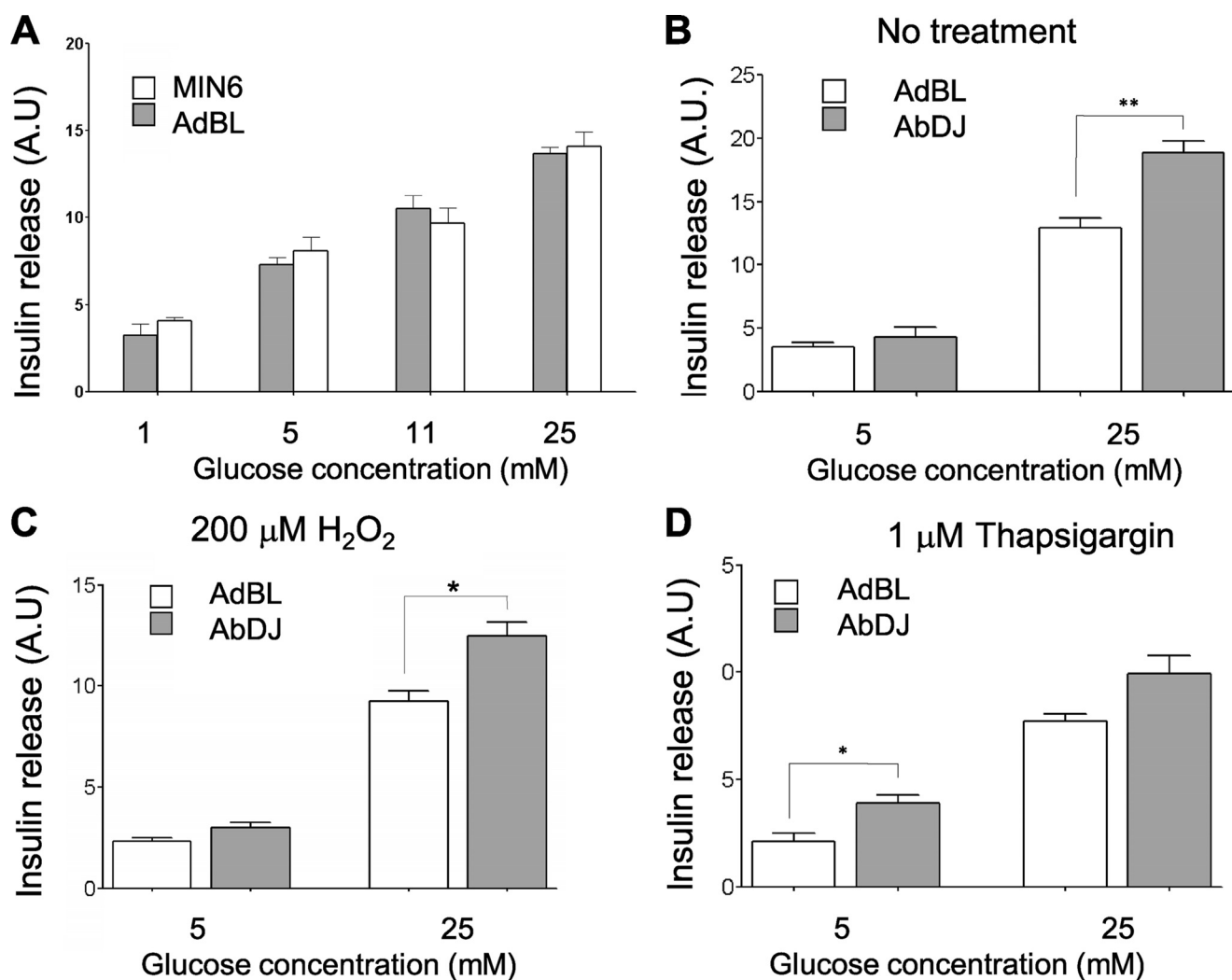
FIGURE 6. **DJ-1 overexpression induces glucose-dependent insulin secretion.** *A*, glucose-induced insulin secretion of naive and AdBL-infected MIN6 cells. 48 h postinfection, the cells were preincubated in KRB/BSA buffer followed by incubation at the indicated glucose concentrations. *B*, insulin secretion of DJ-1-overexpressing MIN6 (AdDJ) or infected with the blank vector (AdBL). Shown is insulin secretion of DJ-1-expressing cells following 200 μM H_2O_2 (*C*) and 1 μM thapsigargin (*D*). The insults were applied for 6 h before glucose-dependent secretion was challenged. Insulin is presented as arbitrary units (*A.U.*) Values are means $\pm$ S.E. (*error bars*), normalized to viable cell number. *, $0.01 < p < 0.05$; **, $0.001 < p < 0.01$, $n = 3$.

secreted was measured (Fig. 6*B*). The same, relative and stress-independent, enhancement of the insulin secretion following a 25 mM glucose stimulus is shown in DJ-1-overexpressing cells exposed to H_2O_2.

We performed a similar series of experiments testing the responsiveness of cells to DJ-1 under the ER stress paradigm. The beneficial effect of DJ-1 on insulin release was pronounced, especially at low concentrations of the stimulant (Fig. 6*C*). This favorable effect takes place despite the severity of the ER stress caused by thapsigargin and the deleterious influence it has on cell viability (see Fig. 5*B*).

DJ-1 Attenuates the ER Stress Response—We proceeded to test the effect of DJ-1 expression on the outcome of the ER stress response. To this end, we tested the expression of BiP (also called GRP78/HSPA5), a key member in the import, folding, and processing of ER proteins. Cells infected by an empty adenovirus vector showed no difference in BiP expression relative to induction achieved by thapsigargin (Fig. 7). However, following infection with DJ-1, the expected increase in BiP was strongly attenuated (Fig. 7). We quantified the effect and found

only a modest elevation in BiP expression (Fig. 7*B*). The restrained elevation in BiP after induction of ER stress suggests that the BiP promoter is only partially induced under conditions of excess DJ-1.

DJ-1 Binds Cytosolic TFII-I—In order to shed light on the mechanism by which DJ-1 participates in the cellular processes and influences β-cell physiology (Figs. 3–6), we assessed the DJ-1-interacting proteins in MIN6 cells. We performed pull-down assays using the FLAG-tagged DJ-1 and applied MALDI-TOF MS to identify the interacting partners. We confidently identified several cytosolic partners, among them PIAS2/Miz1 (UniProt: Q8C5D8), an E3 SUMO-protein ligase that was previously found to bind DJ-1 in transformed cells (18). An interacting band of 110 kDa was isolated and identified with high confidence (MASCOT score 90) to be TFII-I (Fig. 8*A*). This previously unrecognized DJ-1-interacting protein (also called GTF2i; UniProt: Q9ESZ8) belongs to the general transcription factor family II-I (29) that is involved in the mammalian cell cycle and transformation. Recently, TFII-I was shown to play an important role in the regulation of BiP/GPR78 protein as a part

A

AdDJ infection

No treatment   Thapsigargin

-    +   +   -

BiP

Actin

B
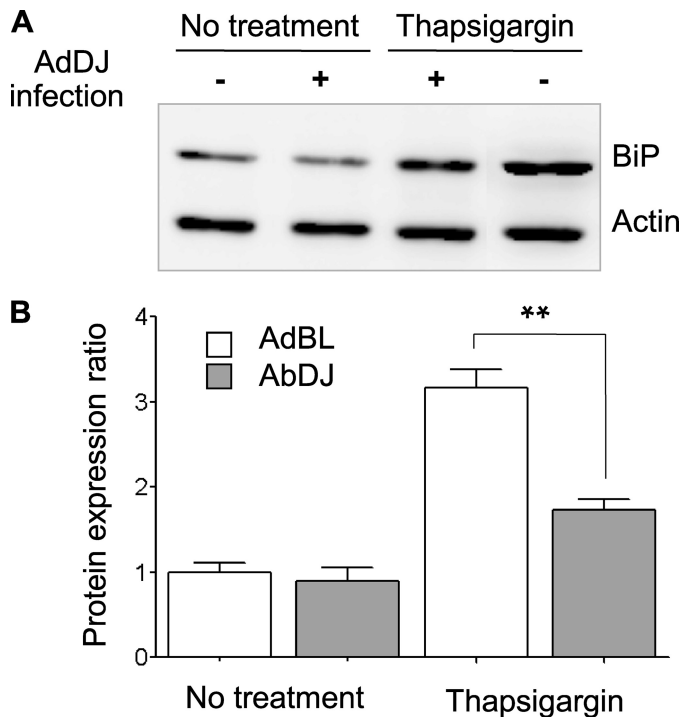
FIGURE 7. **DJ-1 impact on BiP expression.** *A*, BiP induction is attenuated under ER stress in DJ-1-expressing cells. MIN6 cells were infected with AdDJ and treated with 1 μM thapsigargin for 8 h. BiP expression was detected using BiP antibodies. *B*, quantitative results shown are based on three independent experiments. Values are means ± S.E. (*error bars*). *, $0.01 < p < 0.05$; **, $0.001 < p < 0.01$.

of ER stress response (30). In fact, the promoter of BiP (and other genes from the unfolded protein response) is activated by TFII-I (31).

Following stress conditions in MIN6 cells, we identified a moderate up-regulation of TFII-I mRNA (1.5-fold by reverse transcription-PCR). Using immunofluorescent staining, we show that TFII-I is localized mainly to the cytosol, where it is co-localized with DJ-1 (Fig. 8B, *yellow*). Note that a fraction of DJ-1 is already localized to the nucleus prior to any stress condition (Fig. 8B, *green*), whereas staining of TFII-I shows some preference for the plasma membrane (Fig. 8B, *red*). Following oxidative stress, TFII-I is efficiently translocated to the nucleus. However, we observed that in DJ-1-infected cells, the translocation of TFII-I to the nucleus is strongly inhibited in a dose-dependent manner. Specifically, the accumulation of TFII-I in the nucleus is inversely correlated with the fraction of the DJ-1 in the cytosol (Fig. 7, *C* and *D*). In cells that are characterized by high expression of DJ-1, the TFII-I expression remains predominantly in the cytosol. A fraction of the cells (~30%) is characterized as having DJ-1 that is localized only to the nucleus. In these cells, TFII-I was exclusively located in the nucleus following exposure to oxidative stress (Fig. 7, compare *C* and *D*).

DISCUSSION

Chronic exposure to high glucose and free fatty acids leads to deterioration in pancreatic β-cell functionality and mass. The β-cells are under an increased demand for insulin production, proper folding, and packing in secretory granules.

Such demands often cause extensive oxidative and ER stress. The damage to the β-cells reflects their limited ability to cope with these stresses.

Here we identified DJ-1 as a protein that is induced upon chronic exposure to glucose and thus can be considered not only as a sensor for the apparent stress in MIN6 cells but as a molecule that mediates a protection and improved function against multiple stressors. Furthermore, under oxidative stress, a known by-product of glucose load on pancreatic cells, DJ-1 acts to increase cell survival in the face of external insults in pancreatic β-cell lines as well as mouse pancreatic islets. Both experimental systems showed an improved cell viability following oxidative insult, providing an important physiological link between DJ-1 and the ability to cope with stress. Based on our observations, we postulate that modulating DJ-1 levels could potentially attenuate pancreatic β-cell dysfunction and improved survival. Surplus DJ-1 alters the basal state of the cells, rendering them more robust and in a readiness state toward potential insults (Figs. 3–7).

An improved management of pancreatic β-cell line and islets of various stress by a specific combination of cytokines was shown (32). Whereas DJ-1 induction that occurred following oxidative stress (Fig. 1) led to an improved control of oxidative (Fig. 3–5), hyperglycemic (Fig. 6), or ER stress (Fig. 5) in a dose-dependent manner, the exposure of the cells to cytokines (interleukin-1β + interferon-γ) was not associated with a similar induction of DJ-1 (not shown).

In diseased human pancreatic islets it was shown that (i) the glucose-dependent insulin release is severely impaired, and (ii) markers of the unfolded response, such as BiP, are induced by high glucose (33). In our study, an increased level of DJ-1 improved the regulated insulin release (Fig. 6) and rendered the cells less prone to oxidative stress (Fig. 5) and more robust against ER stress as reflected by attenuation of BiP expression (Fig. 7). Insulin release is therefore an indirect measure of the capacity of β-cells to cope with stressful conditions (*i.e.* hyperglycemia). Challenging MIN6 cells experiencing high levels of DJ-1 (excess of 0.5–3-fold) revealed that the level of insulin released under physiological stimulation was significantly increased (~45%; Fig. 6B). This robust increase was not due to a compensatory elevation in insulin mRNA. Actually, MIN6 cells that were infected with DJ-1 seem to strongly attenuate insulin mRNA (up to 40%; data not shown). Furthermore, overexpression of DJ-1 in our experiments significantly attenuated the induction of BiP following induced ER stress (Fig. 7).

A Missing Link between Oxidative and ER Stress—It was noted that protection of β-cells was largely ignored in anti-diabetic therapy. It is thus hypothesized that therapeutic strategies need to act on increasing insulin secretion and decreasing ROS (34). Nonetheless, only a few such molecules are known. Examples are the mTOR and the anti-diabetic PPAR-γ agonists that reduce the load on β-cells (27). However, the beneficial effects are mostly achieved by the action on peripheral insulin-responsive tissues. Here we show that DJ-1 directly affects pancreatic β-cells.

The use of pancreatic β-cell lines as models for T2D is strongly supported. Not only did the cells applied in our study (MIN6 and βTC-6) show that DJ-1 protein is strongly induced
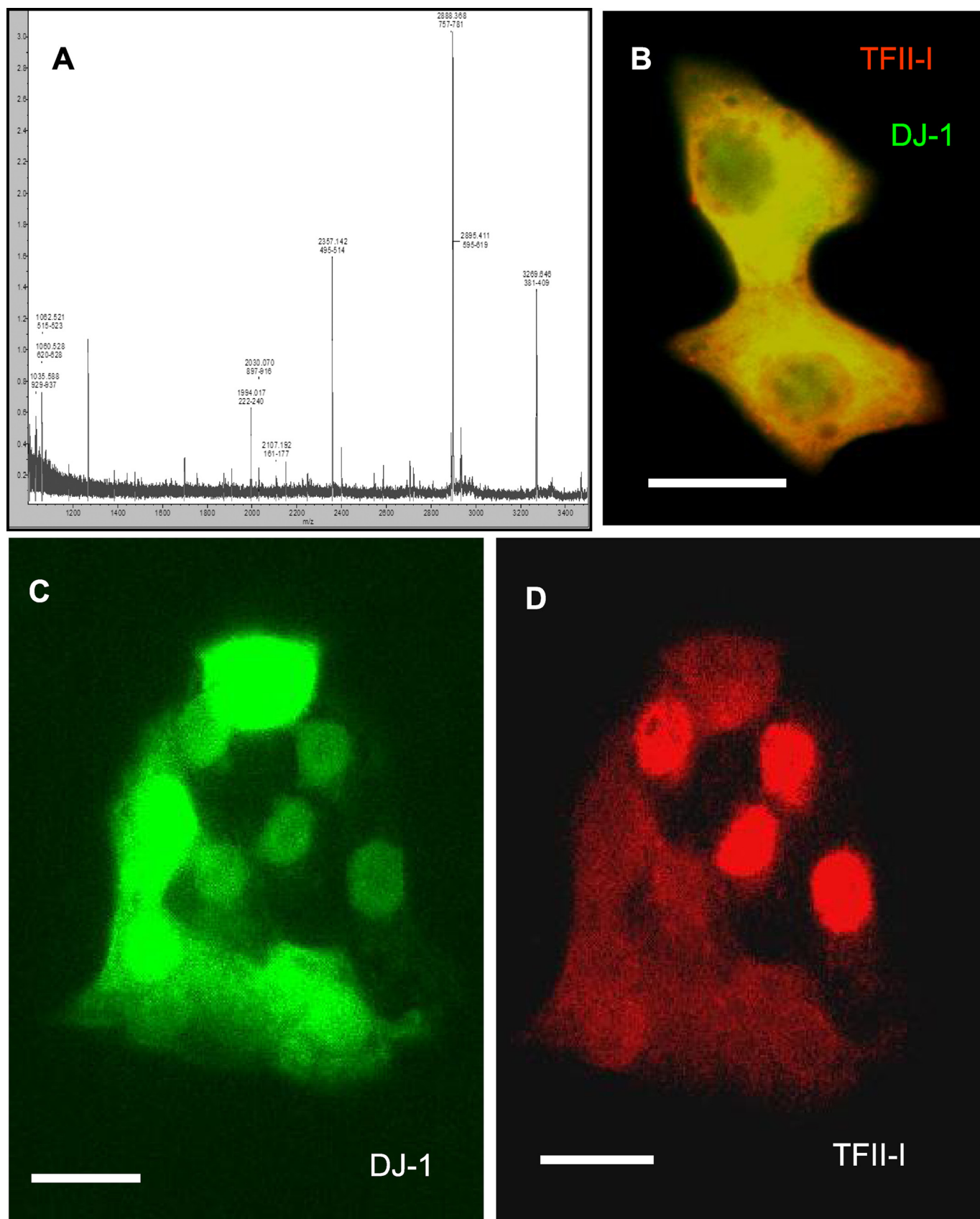
FIGURE 8. **DJ-1-interacting protein TFII-I.** *A*, MALDI-TOF spectrum of a 110-kDa interacting protein. The spectrum shows the peptides that were confidently identified as TFII-I (10 peptides, 18% sequence coverage). The identified peptides are marked with their respective masses. *B*, MIN6-infected cells (AdDJ) under basal conditions were double-stained with antibodies against DJ-1 (Cy3, *green*) and TFII-I (Cy5, *red*). *Yellow*, overlapping in localization. MIN6 cells infected with AdDJ were exposed to 200 μM H_2O_2 (*C* and *D*). The cells were fixed 2 h following the stress and double-stained as above. *Scale bar*, 10 μm.

following oxidative and ER stress (Fig. 2, *A*–*D*, and supplemental Fig. S3); such induction was measured in isolated mouse pancreatic islets. A global proteomic analysis of pancreatic islets found a 1.7-fold induction of DJ-1 under mild stress conditions of short term hyperglycemia and high fat diet (35). It should be noted that regulation by DJ-1 is determined by the absolute amounts and also by the redistribution of DJ-1 between mitochondria, the cytosol, and the nucleus following stress conditions (36).

A large number of studies show that DJ-1 is antioxidant and provides protection in neurons. Nevertheless, the actual mechanism that leads to cell protection is not yet known. In our study, we show that cell protection is not limited to neurons but occurs in a number of pancreatic cellular models. Notably, the amount of DJ-1 is a critical factor in executing this function. We show that down-regulation of DJ-1 (Fig. 3, *B* and *C*) as well as its overexpression (Fig. 3, *D* and *E*) change the ability of the cells to cope with various stress insults. We assume that loss of DJ-1 protein activity or reduction of its amount makes the cells vulnerable to ER stress. The convergence of oxidative and ER stress that is illustrated in this study may result from (i) ER stress causing an elevation in ROS (thus, cells experience elevated oxidative stress conditions) or (ii) ER stress modifying TFII-I and its translocation to the nuclei. Consequently, the subcellular localization and transcriptional activity of DJ-1 is altered, leading to oxidative-like stress transcriptional response. A link between cysteine-sulfinic acid modification of DJ-1 and its subcellular translocation and cell protection properties was proposed (37).

Transcription Regulation by DJ-1 and TFII-I—DJ-1 is expressed in nuclei, mitochondria, and the cytosol (Fig. 8*B*). The wealth of known partners of DJ-1 reflects the complexity and richness of DJ-1 activities. Among the previously identified DJ-1-interacting proteins is PIAS2, a competitor of DJ-1 for androgen receptor regulation (18). TFII-I in itself is a weak transcriptional activator (as is PIAS2), but together they have a strong synergistic effect. We identified TFII-I as a partner of DJ-1 (Fig. 8*A*). We propose that a titration of TFII-I by DJ-1 eventually leads to transcriptional repression. A similar scenario was proposed for the competition for nuclear localization of PIAS2 and TFII-I by MusTRD1/BEN (38).

It is known that DJ-1 regulates the effective levels of ROS, and this activity is reflected by the accumulation of DJ-1-modified isoforms (15). Brain tissues from patients with PD or Alzheimer disease show an accumulation of the oxidized DJ-1 forms (39). Although it is unknown whether the oxidized form of DJ-1 is active in transcription, some effects were attributed to the oxidized isoforms of DJ-1 (40). For example, the oxidized form of DJ-1 but not its unmodified form prevents the transcription of PPAR-γ coactivator (called PGC-1α) (41). Based on the localization studies, we propose that under oxidative stress, the affinity of DJ-1 for TFII-I is decreased, probably due to a new balance between native and modified forms. A short exposure to oxidative conditions in MIN6 (<30 min) was sufficient to cause a modification on the cysteine residue (Fig. 2, *E* and *F*). In this time frame, cell viability is not yet affected possibly indicating that a transcriptional regulation mode is activated.

Our study proposes a molecular link between the biochemical change in DJ-1 (*i.e.* the accumulation of the acidic isoforms; Fig. 2 and supplemental Table S1), transient binding to TFII-I, and translocation of TFII-I to the nucleus (Fig. 8). TFII-I was shown to up-regulate the expression of the anti-apoptotic BiP/GRP78 (Fig. 7), a member of the HSP70 family that is involved in newly synthesized proteins across the ER membrane (31). Competitive binding of ER stress-related transcription factors (such as ATF6 (42) and E2F1 (43)) to TFII-I fully matches a model in which DJ-1 participates in competition for binding to TFII-I. The L166P DJ-1 mutant, which has reduced intrinsic folding (44), showed an improvement of β-cell survival (Fig. 5*A*) similar to that of the wild type DJ-1. We are currently investigating the possibility that despite the difference in overall stability, the binding affinity of the DJ-1 with TFII-I in L166P mutant is comparable with that of the wild type.

Deterioration of β-cells under hyperglycemia is expected to reflect poor management of oxidative and ER stress. An attractive possibility is that DJ-1 and TFII-I provide a transcriptional regulation junction for β-cell protection against multiple stresses. The ER-dependent phosphorylation of TFII-I renders it to an active form that effectively binds to the BiP promoter (30, 31). DJ-1 may be a "coincidence detector" for β-cells that are facing extreme conditions. Within this scheme, it is possible that T2D and other aging-related pathologies reflect the inability of DJ-1 to engage in transcription of genes that that cope with stress response in general.

REFERENCES

1. Poitout, V., and Robertson, R. P. (2002) *Endocrinology* **143,** 339–342
2. Robertson, R. P. (2009) *Trends Endocrinol. Metab.* **20,** 388–393
3. Prentki, M., and Nolan, C. J. (2006) *J. Clin. Invest.* **116,** 1802–1812
4. Brissova, M., Shiota, M., Nicholson, W. E., Gannon, M., Knobel, S. M., Piston, D. W., Wright, C. V., and Powers, A. C. (2002) *J. Biol. Chem.* **277,** 11225–11232
5. Tanaka, Y., Gleason, C. E., Tran, P. O., Harmon, J. S., and Robertson, R. P. (1999) *Proc. Natl. Acad. Sci. U.S.A.* **96,** 10857–10862
6. Wang, H., Kouri, G., and Wollheim, C. B. (2005) *J. Cell Sci.* **118,** 3905–3915
7. Eizirik, D. L., Cardozo, A. K., and Cnop, M. (2008) *Endocr. Rev.* **29,** 42–61
8. Bertolotti, A., Zhang, Y., Hendershot, L. M., Harding, H. P., and Ron, D. (2000) *Nat. Cell Biol.* **2,** 326–332
9. Lin, M. T., and Beal, M. F. (2006) *Nature* **443,** 787–795
10. Lindholm, D., Wootz, H., and Korhonen, L. (2006) *Cell Death Differ.* **13,** 385–392
11. Bonifati, V., Rizzu, P., van Baren, M. J., Schaap, O., Breedveld, G. J., Krieger, E., Dekker, M. C., Squitieri, F., Ibanez, P., Joosse, M., van Dongen, J. W., Vanacore, N., van Swieten, J. C., Brice, A., Meco, G., van Duijn, C. M., Oostra, B. A., and Heutink, P. (2003) *Science* **299,** 256–259
12. Kahle, P. J., Waak, J., and Gasser, T. (2009) *Free Radic. Biol. Med.* **47,** 1354–1361
13. Shendelman, S., Jonason, A., Martinat, C., Leete, T., and Abeliovich, A. (2004) *PLoS Biol.* 10.1371/journal.pbio.0020362
14. Lev, N., Ickowicz, D., Melamed, E., and Offen, D. (2008) *Neurotoxicology* **29,** 397–405

15. Taira, T., Saito, Y., Niki, T., Iguchi-Ariga, S. M., Takahashi, K., and Ariga, H. (2004) *EMBO Rep.* **5,** 213–218
16. Inden, M., Taira, T., Kitamura, Y., Yanagida, T., Tsuchiya, D., Takata, K., Yanagisawa, D., Nishimura, K., Taniguchi, T., Kiso, Y., Yoshimoto, K., Agatsuma, T., Koide-Yoshida, S., Iguchi-Ariga, S. M., Shimohama, S., and Ariga, H. (2006) *Neurobiol. Dis.* **24,** 144–158
17. Kim, R. H., Smith, P. D., Aleyasin, H., Hayley, S., Mount, M. P., Pownall, S., Wakeham, A., You-Ten, A. J., Kalia, S. K., Horne, P., Westaway, D., Lozano, A. M., Anisman, H., Park, D. S., and Mak, T. W. (2005) *Proc. Natl. Acad. Sci. U.S.A.* **102,** 5215–5220
18. Takahashi, K., Taira, T., Niki, T., Seino, C., Iguchi-Ariga, S. M., and Ariga, H. (2001) *J. Biol. Chem.* **276,** 37556–37563
19. Nagakubo, D., Taira, T., Kitaura, H., Ikeda, M., Tamai, K., Iguchi-Ariga, S. M., and Ariga, H. (1997) *Biochem. Biophys. Res. Commun.* **231,** 509–513
20. Kim, Y. C., Kitaura, H., Taira, T., Iguchi-Ariga, S. M., and Ariga, H. (2009) *J. Neurochem.* **110,** 192–192
21. Clements, C. M., McNally, R. S., Conti, B. J., Mak, T. W., and Ting, J. P. Y. (2006) *Proc. Natl. Acad. Sci. U.S.A.* **103,** 15091–15096
22. Junn, E., Taniguchi, H., Jeong, B. S., Zhao, X., Ichijo, H., and Mouradian, M. M. (2005) *Proc. Natl. Acad. Sci. U.S.A.* **102,** 9691–9696
23. Ishihara, H., Asano, T., Tsukuda, K., Katagiri, H., Inukai, K., Anai, M., Kikuchi, M., Yazaki, Y., Miyazaki, J. I., and Oka, Y. (1993) *Diabetologia* **36,** 1139–1145
24. Knaack, D., Fiore, D. M., Surana, M., Leiser, M., Laurance, M., Fusco-DeMane, D., Hegre, O. D., Fleischer, N., and Efrat, S. (1994) *Diabetes* **43,** 1413–1417
25. He, T. C., Zhou, S., da Costa, L. T., Yu, J., Kinzler, K. W., and Vogelstein, B. (1998) *Proc. Natl. Acad. Sci. U.S.A.* **95,** 2509–2514
26. Inberg, A., Bogoch, Y., Bledi, Y., and Linial, M. (2007) *Proteomics* **7,** 910–920
27. Kinumi, T., Kimata, J., Taira, T., Ariga, H., and Niki, E. (2004) *Biochem. Biophys. Res. Commun.* **317,** 722–728
28. Miyazaki, S., Yanagida, T., Nunome, K., Ishikawa, S., Inden, M., Kitamura, Y., Nakagawa, S., Taira, T., Hirota, K., Niwa, M., Iguchi-Ariga, S. M., and Ariga, H. (2008) *J. Neurochem.* 10.1111/j.1471-4159.2008.05327.x
29. Roy, A. L. (2006) *ACS Chem. Biol.* **1,** 619–622
30. Misra, U. K., Wang, F., and Pizzo, S. V. (2009) *J. Cell Biochem.* **106,** 381–389
31. Hong, M., Lin, M. Y., Huang, J. M., Baumeister, P., Hakre, S., Roy, A. L., and Lee, A. S. (2005) *J. Biol. Chem.* **280,** 16821–16828
32. Bast, A., Wolf, G., Oberbäumer, I., and Walther, R. (2002) *Diabetologia* **45,** 867–876
33. Marchetti, P., Bugliani, M., Lupi, R., Marselli, L., Masini, M., Boggi, U., Filipponi, F., Weir, G. C., Eizirik, D. L., and Cnop, M. (2007) *Diabetologia* **50,** 2486–2494
34. Bonora, E. (2008) *Nutr. Metab. Cardiovasc. Dis.* **18,** 74–83
35. Waanders, L. F., Chwalek, K., Monetti, M., Kumar, C., Lammert, E., and Mann, M. (2009) *Proc. Natl. Acad. Sci. U.S.A.* **106,** 18902–18907
36. Junn, E., Jang, W. H., Zhao, X., Jeong, B. S., and Mouradian, M. M. (2009) *J. Neurosci. Res.* **87,** 123–129
37. Canet-Avilés, R. M., Wilson, M. A., Miller, D. W., Ahmad, R., McLendon, C., Bandyopadhyay, S., Baptista, M. J., Ringe, D., Petsko, G. A., and Cookson, M. R. (2004) *Proc. Natl. Acad. Sci. U.S.A.* **101,** 9103–9108
38. Tussie-Luna, M. I., Michel, B., Hakre, S., and Roy, A. L. (2002) *J. Biol. Chem.* **277,** 43185–43193
39. Choi, J., Sullards, M. C., Olzmann, J. A., Rees, H. D., Weintraub, S. T., Bostwick, D. E., Gearing, M., Levey, A. I., Chin, L. S., and Li, L. (2006) *J. Biol. Chem.* **281,** 10816–10824
40. Ishikawa, S., Taira, T., Niki, T., Takahashi-Niki, K., Maita, C., Maita, H., Ariga, H., and Iguchi-Ariga, S. M. (2009) *J. Biol. Chem.* **284,** 28832–28844
41. Zhong, N., and Xu, J. (2008) *Hum. Mol. Genet.* **17,** 3357–3367
42. Parker, R., Phan, T., Baumeister, P., Roy, B., Cheriyath, V., Roy, A. L., and Lee, A. S. (2001) *Mol. Cell Biol.* **21,** 3220–3233
43. Racek, T., Buhlmann, S., Rüst, F., Knoll, S., Alla, V., and Pützer, B. M. (2008) *J. Biol. Chem.* **283,** 34305–34314
44. Moore, D. J., Zhang, L., Dawson, T. M., and Dawson, V. L. (2003) *J. Neurochem.* **87,** 1558–1567